

Deep dry-etch of silica in a helicon plasma etcher for optical waveguide fabrication

W. T. Li,^{a)} D. A. P. Bulla, J. Love, and B. Luther-Davies

Australian Photonics CRC, Research School of Physical Sciences and Engineering,
The Australian National University, ACT 0200, Australia

C. Charles and R. Boswell

Plasma Research Laboratory, Research School of Physical Sciences and Engineering,
The Australian National University, ACT 0200, Australia

(Received 25 August 2004; accepted 8 November 2004; published 15 December 2004)

Dry-etch of SiO₂ layers using a CF₄ plasma in a helicon plasma etcher for optical waveguide fabrication has been studied. Al₂O₃ thin films, instead of the conventional materials, such as Cr or photoresist, were employed as the masking materials. The Al₂O₃ mask layer was obtained by periodically oxidizing the surface of an Al mask in an oxygen plasma during the breaks of the SiO₂ etching process. A relatively high SiO₂/Al₂O₃ etching selectivity of ~100:1, compared with a SiO₂/Al selectivity of ~15:1, was achieved under certain plasma condition. Such a high etching selectivity greatly reduced the required Al mask thickness from over 500 nm down to ~100 nm for etching over 5- μ m-thick silica, which make it very easy to obtain the mask patterns with near vertical and very smooth sidewalls. Accordingly, silica waveguides with vertical sidewalls whose roughness was as low as 10 nm were achieved. In addition, the mechanism of the profile transformation from a mask to the etched waveguide was analyzed numerically; and it was found that the slope angle of the sidewalls of the mask patterns only needed to be larger than 50° for achieving vertical sidewalls of the waveguides, if the etching selectivity was increased to 100. © 2005 American Vacuum Society. [DOI: 10.1116/1.1842114]

I. INTRODUCTION

Silica-based channel waveguides are potential building blocks of planar lightwave circuits for future optical telecommunication systems. The key step in the fabrication process of the waveguides is the deep dry-etch of the silica (~5–10 μ m thick). To realize vertical and smooth sidewalls of such thick waveguides is always a big challenge, because a thick etching mask is required, and the mask fabrication processes (lithograph, wet-etch, and dry etch), always generate certain roughness and slope to the sidewalls of the mask patterns, which are then transferred to the etched underlying silica layer. Much research efforts have been spent on reducing the sidewall roughness of the waveguides in the last decade, since the roughness causes significant optical scattering loss of the propagating wave power in the waveguides.^{1–6}

Different masking materials for etching the silica waveguide, such as chromium,^{1,2} amorphous silicon (*a*-Si),^{3,4} AlSi,⁵ and photoresist,^{4,6} have been reported. The sidewall roughness of the waveguide achieved using above masking materials is usually between 20 and 150 nm. The Cr is the most widely used one, because it enables a very high SiO₂/Cr etching selectivity (20:1–70:1), which is much higher than that of the SiO₂/*a*-Si (~15:1), SiO₂/AlSi (~10:1), or SiO₂/resist (~5:1).

The Cr masks with a thickness of 200–500 nm are normally required for etching the silica waveguides. To obtain such thick Cr masks whose patterns have vertical and very

smooth sidewalls is very difficult. A lift-off process is usually not applicable for patterning a thick Cr layer (>200 nm), because of the chromium's high hardness and strong adhesion to photoresist and silica. Wet-etch using photoresist as the masking material is a convenient method for patterning the Cr masks, but the generated Cr patterns always have rough edges and slanted sidewalls, due to mainly an inevitable uneven undercutting mechanism of the wet-etching process. Dry-etching a thick Cr metal layer requires expensive reactant gases, and a very strong etching mask made of, such as *a*-Si, instead of photoresist. The processing steps for the mask fabrication is thus increased compared with the wet-etch technique, and more roughness could be induced to the final Cr mask. Focused ion beam etching with an Ar plasma can be used to fabricate the Cr masks, but it is obviously not efficient, and it causes some unwanted etching effects to the samples.^{1,7}

In this work, Al₂O₃ thin films were studied as the masking material. To fabricate an Al₂O₃ mask whose patterns have vertical and very smooth sidewalls was also found to be very difficult using the conventional techniques. A special method was therefore developed for obtaining the Al₂O₃ mask. In this method, the Al₂O₃ mask was generated by periodically oxidizing the surface of an Al metal mask using an O₂ plasma during the breaks of the silica etching process. The Al₂O₃ layer was found to offer an extremely high SiO₂/Al₂O₃ etching selectivity of ~100:1, which was much higher than the SiO₂/Al selectivity of ~15:1 at the same plasma condition. Thus a very thin Al₂O₃ mask (70–100 nm), rather than a thick Cr (>200 nm) or Al (>500 nm)

^{a)}Electronic mail: weitang.li@anu.edu.au

mask, was enough for etching over 5- μm -thick SiO_2 , and the Al_2O_3 mask could be obtained from an Al mask of similar thickness. Such a reduction of the mask thickness greatly reduced the fabrication processes induced roughness to the mask, and provided the possibility to accurately control the linewidth of the masks and the waveguides. In addition, Al is much more reactive and softer than the Cr, making it easier to be patterned than the Cr using the routing dry-etch or lift-off techniques well developed in integrated circuits processing. As a consequence, silica optical waveguides with vertical and very smooth sidewalls (roughness ~ 10 nm) were easily achieved. In comparison, when a thick Al masks fabricated using wet-etch process was applied for the waveguide etching, and the surface of the mask was not oxidized, the obtained waveguides exhibit slanted sidewalls with a roughness of over 100 nm. The details of the earlier work and some results are presented in the following.

II. EXPERIMENT

The dry-etch was carried out in a helicon plasma etcher, which has been detailed elsewhere.⁸ Briefly, it consists of two joined chambers, the source and diffusion chambers. The source chamber is a 15 cm diameter, 25 cm long glass tube surrounded by a Boswell-type helicon antenna and two solenoids. The diffusion chamber is a 30 cm diameter and 30 cm long aluminum cylinder surrounded by two additional solenoids. The currents in the four solenoids are adjusted to produce a magnetic field of 100 G in the source and 60 G in the diffusion chamber. The substrate holder is mounted at the bottom of the diffusion chamber, and is water cooled. Both the source antenna and the substrate holder are driven by 13.56 MHz radio frequency (rf) power sources. The chambers are pumped with an ATP 400 HPC turbo molecular pump. The processing gases of O_2 , Ar, and CF_4 are admitted into the vacuum chamber through 3 separate mass flow controllers.

The silica thin films (5–7 μm thick) to be etched were produced using a helicon plasma activated reactive evaporation technique.^{9,10} The original Al masks were ~ 100 nm thick, and were patterned using a lift-off process. For comparison, 500-nm-thick Al metal masks were also fabricated on some samples using a wet-etching process with the etchant of $\text{H}_3\text{PO}_4:\text{HNO}_3:\text{HAc}:\text{H}_2\text{O}=16:1:1:2$.

The plasma etching of the silica was not performed continuously, but was periodically intervened for oxidizing the surface of the Al masks in an oxygen plasma. The etching duration (1–2 min) of the silica was set to keep the etched Al_2O_3 thickness to be less than the grown during each of the period from the Al_2O_3 growth to the silica-etch. For some samples masked with the 500-nm-thick Al, the etching was done continuously without the oxidation of the mask surface.

An *in situ* variable angle spectroscopic ellipsometry (VASE) was employed for testing the growth rate of the Al_2O_3 layers from the surface of the Al. Very thin Al layers (~ 20 nm) deposited on Si wafers were applied, so that the Al layers were nearly transparent in visible lights, and very accurate thickness of the Al_2O_3 and Al could be measured

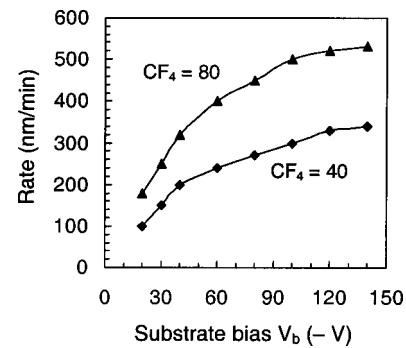


Fig. 1. Etch rate of SiO_2 as a function of substrate bias V_b for the cases of CF_4 flow at 40 and 80 sccm, respectively, when keeping a plasma power of 1000 W.

using the VASE. The growth rate of the Al_2O_3 was found to increase with the plasma power, but decrease with the increase of the substrate bias due to a sputtering effect. A 7–9-nm-thick pure Al_2O_3 layer could be obtained in 2 min using the optimized O_2 plasma conditions of plasma power 1000 W, substrate rf power 0 W, and processing gas pressure 2 mTorr.

The etch rates of the SiO_2 and the masking materials (Al and Al_2O_3) were measured *in situ* using the ellipsometry, and *ex situ* using a surface profilometer. The microprofiles of the masks and the waveguides were investigated under a field emission scanning electron microscopy (FESEM). The sidewall roughness of waveguides was determined by measuring the average amplitude of the corrugations or ripples within a 2 μm range on the sidewalls using the FESEM.

III. RESULTS AND DISCUSSIONS

A. Etch rate of SiO_2

The etch rate of the silica as a function of the applied substrate bias (V_b) for different CF_4 flow rates was displayed in Fig. 1. The helicon plasma power (P) was 1000 W, and the CF_4 flow rate was 40 or 80 sccm, which generating a processing gas pressure of 1 or 2 mTorr, respectively. The substrate bias V_b was measured as the average voltage of the substrate rf power. It is seen from Fig. 1 that the etch rate increases roughly linearly with V_b when V_b is lower than 120 V. This is due to that the ion bombardment energy increases with V_b , and the silica-etch is an ion bombardment dominated process.¹¹ The ion bombardment not only provides a physical sputtering effect for the etching, but also accelerates the chemical reaction at the silica surface. The total ion bombardment potential included both V_b and the plasma potential (~ 20 – 30 V). Therefore, even at a low V_b of -25 V, a high etch rate of ~ 200 nm/min still could be obtained in the case of using a CF_4 flow of 80 sccm, as shown in Fig. 1. The decrease of the etch rate when reducing the CF_4 flow from 80 to 40 sccm was related to the decrease of the flux of the reactive radicals including ions and neutrals.

In Fig. 2, the etch rate of the silica is plotted versus the helicon plasma power (P) for the cases of no Ar addition and adding a 5 sccm Ar flow to the processing gas, respectively,

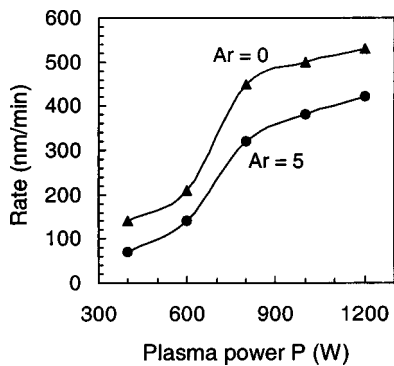


FIG. 2. Etch rate of SiO₂ vs the helicon plasma power for the cases of no Ar addition and adding an Ar flow of 5 sccm to the processing gas, respectively, when keeping $V_b = -100$ V, and CF₄ flow 80 sccm.

while keeping a CF₄ flow at 80 sccm, and $V_b = -100$ V. It is seen here that the etch rate increases with P , due to the increase of the ion flux to the substrate. The operation of the helicon reactor can transit from a capacitive to an inductive to a helicon discharge mode when increasing P , leading to the plasma density and the dissociation rate of the CF₄ gas increase correspondingly.¹² At a power of over 1000 W, the plasma was working in the helicon discharge mode, and thus a very high etching rate of over ~ 500 nm/min was obtained in the case of no Ar addition. The decrease of the etch rate when adding Ar to the processing gas, as shown in Fig. 2, was caused possibly by a dilution effect of the Ar to the CF₄ gas. Therefore, the addition of Ar to the CF₄ gas was not applied for etching the waveguide with the helicon plasma etcher.

It is worthwhile to mention that, as measured by using the *in situ* ellipsometer, there were no detectable polymer layers deposited on the samples during the etching. The reason for this was that the substrate temperature was relatively high (~ 30 – 50 °C), and the processing gas pressure was very low (1–2 m Torr) in our case, so that the deposited polymer layer could be too thin (< 1 nm) to be detected. This could be of benefit to the reduction of the sidewall roughness of the etched waveguide, since a thick polymer layer deposited on the sidewalls could induce a micromasking effect, which is a possible fact to cause the sidewall roughness of the etched waveguides.⁴

B. Etching selectivity

Figure 3 exhibits the variations of the etch rates of the Al and Al₂O₃, as well as the SiO₂/Al₂O₃ and SiO₂/Al etch rate ratios, namely etching selectivities, versus the substrate bias V_b when keeping $P = 1000$ W and the CF₄ flow at 80 sccm. As shown in the figure, the etch rates of both Al and Al₂O₃ increase, but the SiO₂ etching selectivities over the both decrease, with the increase of V_b ; and the SiO₂/Al₂O₃ selectivity is much higher than that of the SiO₂/Al at low bias. These indicate that, at low bias (< 50 V), the Al₂O₃ is much more inert than the Al to the reactive species coming from the CF₄ plasma, so that the etch rate of the Al₂O₃ is much lower than that of the Al; but when increasing the bias further, ion sput-

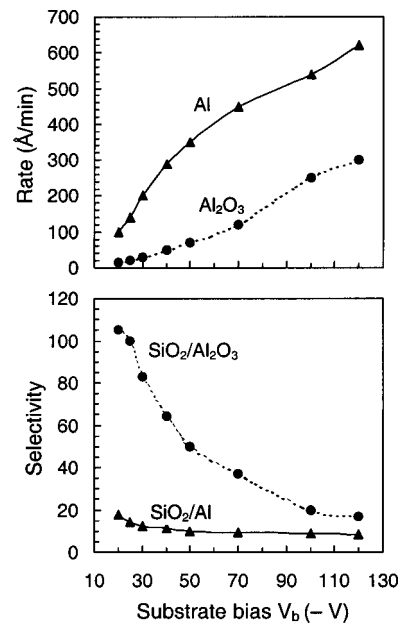


FIG. 3. Etch rates of Al and Al₂O₃, and the etching selectivities of SiO₂/Al₂O₃ and SiO₂/Al, vs the V_b when keeping $P = 1000$ W and the CF₄ flow at 80 sccm.

tering effect may become dominating for the etch of the both, leading to the etch rates of the both increase rapidly, and the etching selectivities over the both decrease.

Based on the experimental data showing in Fig. 3, suitable conditions can be chosen for etching the waveguides. For example, we could choose $V_b = -25$ V, $P = 1000$ W, and CF₄ flow 80 sccm for the SiO₂ etching, and set both the SiO₂ etch and the Al₂O₃ growth periods to be 2 min, while using the optimized parameters for the surface oxidation of the Al mask as stated previously in Sec. II, so that an extremely high SiO₂/Al₂O₃ etching selectivity of $\sim 100:1$ is obtained, and the etched Al₂O₃ thickness (~ 4 nm) is less than the grown (~ 7 nm) during each of the cycle from the Al₂O₃ growth to SiO₂ etch to Al₂O₃ growth. In addition, if these processing conditions are applied, there is no need to retune the matching conditions of the helicon plasma when switching between the Al₂O₃ growth and SiO₂ etch, since the applied helicon plasma power (1000 W) and processing gas pressure (2 mTorr) are the same in both cases.

C. Microprofiles of the waveguides

The micrographs of 6- μ m-thick silica waveguides obtained using the processing conditions discussed above were displayed in Fig. 4(C) and 4(E), where the applied Al masks produced using the lift-off process have been removed. As seen from the figure, vertical and very smooth sidewalls of the waveguides were achieved. Whereas, although the same processing conditions were applied, the waveguide obtained using the wet-etched Al mask (500 nm thick) exhibit slanted and rough sidewalls, as shown in Fig. 4(D). The difference of these two kinds of waveguides should be attributed to the difference of the original Al masks. The lift-off process produced Al mask patterns (100 nm thick) normally possessed

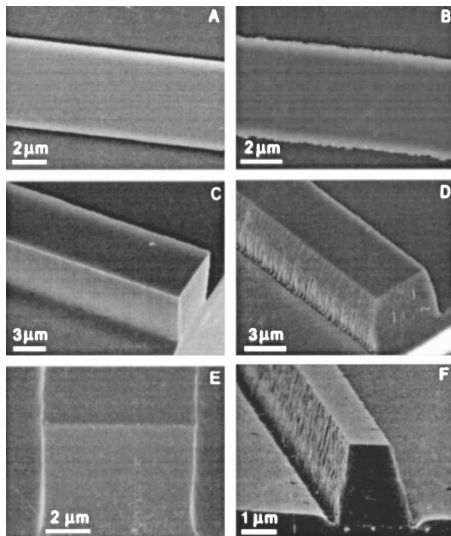


FIG. 4. A and B are the micrographs of the Al mask patterns obtained using the lift-off and wet-etch process, respectively; C and D are the micrographs of the waveguides etched under the mask A and B, respectively, the mask surfaces were oxidized during etching; E is the cross section of the waveguide C; F is also a waveguide etched under mask B, but without surface oxidation to the mask.

near vertical sidewalls and very smooth edges, as shown in Fig. 4(A); but the wet-etched Al patterns always had quite slanted sidewalls and rough edges, as shown in Fig. 4(B), due to an uneven undercutting mechanism of the wet-etch process. The different profile and roughness of the masks were then transferred to the related waveguides during the dry-etch process.

Figure 5 illustrates the mechanism of the profile transformation from a mask to a dry-etched waveguide. In this figure, the cross section of the original etching mask is represented by the shape of ABCD, whose slope angle is α ; the mask is assumed to be eroded evenly down a depth of EE' ($EE'=BB'=CC'=FF'$) after the silica is etched down a depth of AA' , leading to the shapes of the mask and the waveguide become $E'B'C'F'$ and $A'E'F'D'$, respectively. Here, the effect of the angular dependence of sputtering yield on ion incidence angle is neglected, and it is assumed that the plasma etch to the mask and silica occurs only along the

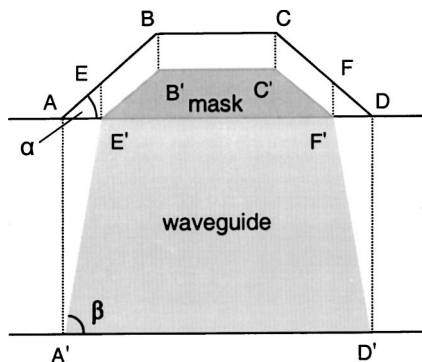


FIG. 5. Mechanism of the sidewall slope transformation from a mask to a dry-etched waveguide.

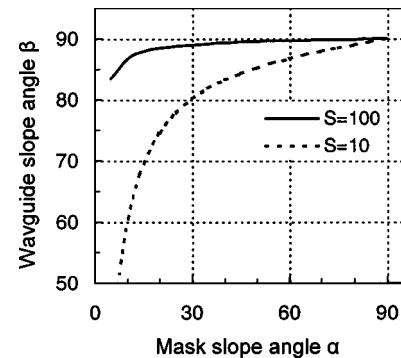


FIG. 6. Dependence of the waveguide slope angle β , plotted according to Eq. (1), on the slope angle α of the mask for the cases of $S=100$ and 10 , respectively.

direction vertical to the sample surface; in another words, there is no side-etching. This is nearly true for the helicon plasma etcher when it operates at very low processing pressure (1–3 mTorr). Therefore, based on Fig. 5, the slope of the waveguide can be written as

$$\tan(\beta) = S \cdot \tan(\alpha), \quad (1)$$

where β is the slope angle of the sidewall of the waveguide, and S is the etching selectivity ($S=AA'/EE'$). The dependence of β on α for different S , according to Eq. (1), is plotted in Fig. 6. It is seen that in the case of $S=100$, as for using the Al_2O_3 as the masking material, β is less dependent on α , and it begins to approach 90° when α goes over 50° , implying that the tolerance of the deviation of α from 90° is very large ($\sim 40^\circ$) for achieving a β of $\sim 90^\circ$. This is very important for realizing vertical sidewall of the waveguide, since it is not easy, in practice, to obtain an Al mask whose α equals exactly to 90° , even with the lift-off or dry-etch process. In our experiment, the α of the Al patterns obtained using the lift-off process was measured under the FESEM, and was found to be 60° – 80° . The achievement of the vertical sidewalls of the related waveguides needs therefore to be explained by not only the high β value of the masks but also by the high etching selectivity.

In addition, Fig. 6 also shows that in the case of $S=10$, as for using Al as the masking material, α plays an important role to affect β , and any deviation of α from 90° will lead to a slanted sidewall of the obtained waveguide. As an example, a silica layer masked with the 500-nm-thick wet-etched Al was etched continuously down to a depth of $3 \mu\text{m}$ under the plasma conditions of $P=1000 \text{ W}$, $V_b=-70 \text{ V}$, and CF_4 flow at 80 sccm, so that only a low selectivity of $S \sim 10$ was obtained. The generated waveguide appeared to have obviously a slanted sidewall with a β of $\sim 81^\circ$, as shown in Fig. 4(F). It was known roughly from the FESEM measurements that the α of the wet-etched Al patterns was between 30° and 40° . Thus the β of the waveguide should be between $\sim 80^\circ$ and 83° according to Eq. (1), which is in good agreement with the experimental result.

From the earlier analysis to the mechanism of the slope transformation from a mask to a waveguide, as indicated in

Fig. 5, we can also foresee that any irregularity along the edges at the bottom of the mask pattern, or on the surface of the sidewall of the mask pattern can be transferred to the sidewalls of the generated waveguide. Therefore the original smoothness of the Al mask is the primary fact to decide the sidewall roughness of the etched waveguide. Usually the thinner the Al mask, the smoother the obtained sidewalls and edges of the mask patterns using no matter lift-off, wet-etch, or dry-etch process. Whereas, the thinner of the etching mask, the higher the etching selectivity is required. Therefore, a high etching selectivity is not only important for realizing vertical sidewalls of the waveguides, but is also essential for obtaining smooth sidewalls of the waveguides.

The sidewall roughness of the waveguides, measured using the FESEM, was around 10, 100, or 150 nm for the three different waveguides shown in Figs. 4(C), 4(D), and 4(F), respectively. This indicated that there was a great improvement of the sidewall smooth of the waveguides, when the applied etching mask was changed accordingly as described earlier or in the figure caption.

IV. CONCLUSIONS

In summary, dry-etch of silica with a helicon plasma etcher for optical waveguide fabrication has been studied. A very simple method for realizing vertical and very smooth sidewalls of the waveguides was demonstrated. Al_2O_3 thin films grown from the surface of Al masks were studied as the mask layers for etching the waveguides. An extremely high $\text{SiO}_2/\text{Al}_2\text{O}_3$ etching selectivity of $\sim 100:1$, in comparing with a SiO_2/Al selectivity of $\sim 15:1$ at the same plasma conditions, was achieved. Such a high etching selectivity greatly reduced the required mask thickness down to ~ 100 nm, which made it easy to obtain high quality mask patterns, and resulted in the achievement of vertical and very smooth sidewalls of the waveguides. In addition, the mechanism of the profile transformation from a mask to the etched

waveguide was analyzed; and it was found that increasing the etching selectivity is not only important for realizing vertical sidewalls of the waveguides, but is also essential for obtaining smooth sidewalls of the waveguides.

The demonstrated waveguide fabrication method is highly desirable for the manufacture of integrated optical circuits or device based on silica waveguides for future optical telecommunication application, since the Al masks can be produced using the routing dry-etch or lift-off techniques well developed in integrated electronic circuits processing. In particular, this method could be a very good choice in the case of the linewidth of the waveguide needs to be controlled accurately.

ACKNOWLEDGMENT

The authors are grateful to Dr. Cheng Huang in the Electronic Microscope Unit of ANU for giving assistance with the FESEM application.

¹A. K. Dutta, *Jpn. J. Appl. Phys.*, Part 1 **34**, 365 (1995).

²K. J. An, D. H. Lee, J. B. Yoo, J. Lee, and G. Y. Yeom, *J. Vac. Sci. Technol. A* **17**, 1483 (1999).

³M. V. Bazylenko, M. Gross, and M. Faith, *Appl. Phys. Lett.* **69**, 2178 (1996).

⁴M. V. Bazylenko, and M. Gross, *J. Vac. Sci. Technol. A* **14**, 2994 (1996).

⁵B. Kim, K. H. Pkwon, and S. H. Park, *J. Vac. Sci. Technol. A* **17**, 2593 (1999).

⁶C. Dominguez, J. Munoz, R. Gonzalez, and M. Tudanca, *Sens. Actuators, A* **38**, 779 (1993).

⁷K. Wang, P. Filloux, N. Paraire, P. R. Cabarrocas, and P. Bulkin, *J. Vac. Sci. Technol. B* **21**, 966 (2003).

⁸A. Herrick, A. J. Perry, and R. Boswell, *J. Vac. Sci. Technol. A* **21**, 955 (2003).

⁹W. T. Li, D. A. P. Bulla, C. Charles, R. Boswell, J. Love, and B. Luther-Davies, *J. Vac. Sci. Technol. A* **21**, 792 (2003).

¹⁰D. A. P. Bulla, W. T. Li, C. Charles, R. Boswell, A. Ankiewicz, and J. Love, *Appl. Opt.* **43**, 2978 (2004).

¹¹S. T. Jung, H. S. Song, D. S. Kim, and H. S. Kim, *Thin Solid Films* **341**, 188 (1999).

¹²P. Chabert, *J. Vac. Sci. Technol. B* **19**, 1339 (2001).